Supplement of Atmos. Chem. Phys., 26, 9827–9855, 2026
https://doi.org/10.5194/acp-26-9827-2026-supplement

Atmospheric Chemistry and Physics
Open Access

Supplement of

Pollution transport and transformation over the Po Plain as revealed by airborne and ground-based measurements in July 2017 during EMeRGe

Costanza Civale et al.

Correspondence to: Maria Dolores Andrés Hernández (lola@iup.physik.uni-bremen.de)

S1 Population density of the Po Valley

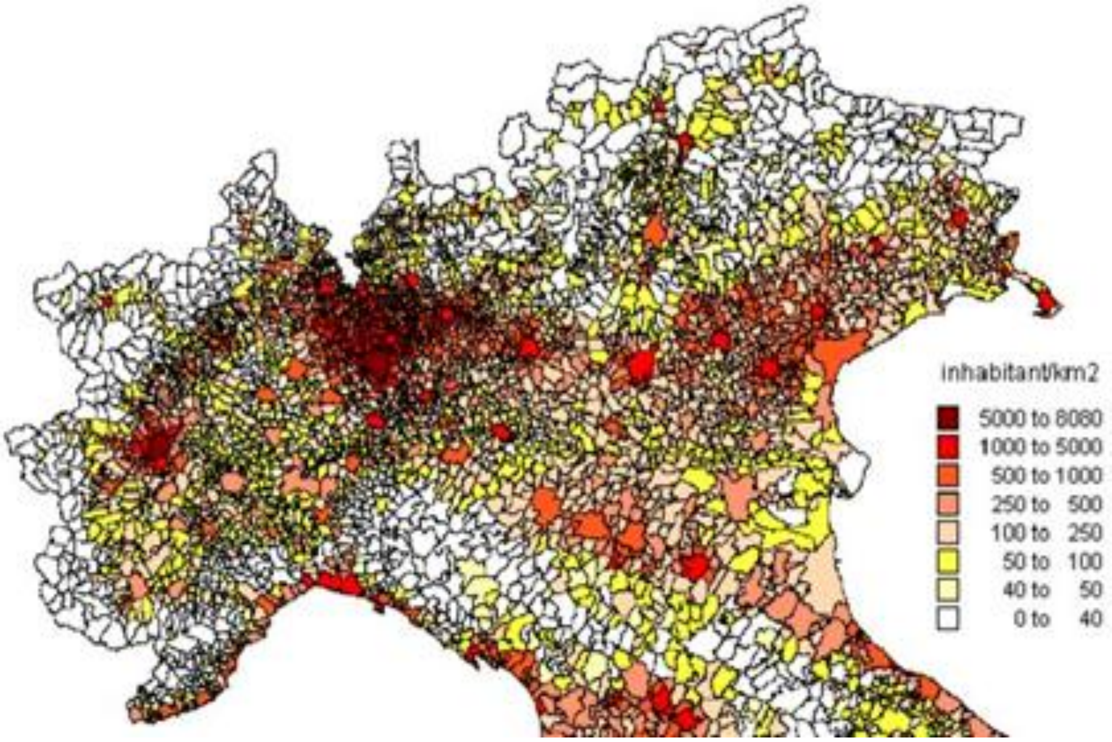

Figure S1. Population density of the Po Valley region. The most populated areas are Milan (north, north-west) and Turin (west). Source: Baklanov and Mahura, 2010.

S2 Emission sources of pollutants in the Po Valley

Table S1. Percentage of the different emission sources classified by macro-sectors (MS) for the Po Valley, 2013. Source: Raffaelli et al. (2020).

Macro-sectors	NH_3	Non-Methane Organic Compound (NMVOC)	NMVOC without MS10and MS11	NO_x	PM_{10}	SO_2
MS1—Combustion in energy and transformation industries	0%	0%	0%	6%	1%	18%
MS2—Non-industrial combustion plants	0%	5%	11%	9%	56%	7%
MS3—Combustion in manufacturing industry	0%	1%	2%	15%	4%	41%
MS4—Production processes	0%	4%	9%	3%	3%	21%
MS5—Extraction and distribution of fossil fuel and geothermal energy	0%	2%	4%	0%	0%	0%
MS6—Solvent and other product	0%	28%	58%	0%	5%	0%
MS7—Road transport	1%	6%	14%	50%	20%	1%
MS8—Other mobile sources and machinery	0%	1%	2%	13%	4%	10%
MS9—Waste treatment and disposal	1%	0%	0%	1%	0%	2%
MS10—Agriculture	97%	22%	0%	1%	4%	0%
M11—Other sources and sinks	0%	31%	0%	0%	3%	0%
Total Emissions	100%	100%	100%	100%	100%	100%

S3 International studies investigating pollution pathways over the Po Valley

- The TRANSALP project was carried out as part of EUROTRAC/TRACT 1989-1991 (European Experiment on Transport and Transformation of Environmentally Relevant Trace Constituents in the Troposphere over Europe/ Transport of Air Pollutants over Complex Terrain). It comprised three tracer field experiments (1989, 1990, and 1991) performed in the south of Switzerland to evaluate the meso-scale transport and diffusion of pollutants across the Alps. The experiments studied the complex mountain topography, focusing on the mountain-plain circulation system and the meteorological conditions that favour the exchange of transalpine air masses and proved the occurrence of transport in the south-north direction (Ambrosetti et al., 1998).

- The PIPAPO (Pianura Padana Produzione di Ozono) campaign (May-June 1998) was part of the EUROTRAC-2 LOOP (Limitation Of Oxidant Production) subproject and combined airborne and ground-based measurements with chemical transport models to analyse VOC/NO_x sensitivity of O_3 production in the Milan plume and pollutants dispersion in the surrounding region. The results of PIPAPO showed the recirculation of polluted air masses in the emission area of Milan, after their injection in the mountain valleys. No evidence of transalpine flow of pollution was found during the project. However, as this study specifically targeted the surroundings of Milan and not the neighbouring regions and was restricted to the late spring months of May and June, it cannot be considered representative for the Po Plain dispersion of pollutants (Neftel et al., 2002; Dosio et al., 2002).

- EU FP7 projects MEGAPOLI and CityZen included the Po Plain among the investigated major population centres (MPCs). The two projects took place in the period 2008-2011 to assess the effect of MPC emissions on a larger scale and investigate the exchange with the neighbouring regions (Baklanov, 2010; Gauss, 2011). MEGAPOLI showed that under anti-cyclonic conditions, the Po Plain footprint extends to southern Europe and northern Italy, while larger urban agglomerates like Milan are responsible for high levels of $PM_{2.5}$ inside the region (Baklanov, 2010).

- The APPRAISAL survey (2011-2014) was a further instrument of the EU FP7 to investigate air quality management in Europe. A section of the project dealt with the Po Plain region Emilia-Romagna and listed the abatement strategies for NH_3, NO_x and PM_{10} (Belis et al., 2017).

- In 2017, EU LIFE-IP Clean Air PREPAIR (Po Regions Engaged to Policies of Air; https://www.lifeprepair.eu/, last access: 06.Juni.2026) started after the stipulation of an agreement between the governments of Italy and Slovenia, the administrative Po Plain regions, and their environmental organisations. Slovenia was involved in the project in order to extend the air pollution management to the Adriatic Sea area. The objectives of LIFE-IP-PREPAIR are the reduction of pollution levels in the Po Plain through the implementation of abatement strategies and the evaluation of their effectiveness. Another aim of the project is to raise the environmental awareness in the community and create a network at the national and regional level between researchers, political and socio-economical entities. The project was due to end in 2024 (Raffaelli et al., 2020, Marongiu et al., 2022).

- RI-URBANS (2021-2025, https://riurbans.eu, last access: 05 October 2025) is a H2020 Green Deal Project that integrates European air quality monitoring networks with research infrastructures (RI), e.g., ACTRIS, ICOS, IAGOS, to enhance real-time observations of atmospheric pollutants, including aerosols. The Po Valley is a key pilot area where advanced monitoring techniques are tested to assess air pollution exposure, with specific activities in Milan and Bologna focusing on black carbon, particulate matter composition, and urban pollution sources (Apituley et al., 2024). Among the large number of city targets studied, the investigation in Milan focused specifically on the effect of the emissions of the airport Milano Linate in the urban area (Magnani et al., 2024).

- TEAMx (Rotach et al, 2022; https://www.teamx-programme.org/, last access: 05 October 2025) investigates atmospheric exchange processes over mountainous regions, with some observational campaigns extending to areas near the Po Valley. Within TEAMx, microscale flows resulting from boundary layer dynamics in the Alp valleys were investigated and the results shown to be very site dependent Using ground-based, remote sensing, and aircraft measurements, the initiative helps improve the understanding of boundary layer dynamics and transport processes, which influence aerosol distribution and air quality in the surrounding regions.

- MAIA (Diner et al; 2018; https://maia.jpl.nasa.gov; last access: 05 October 2025) is a partnership between NASA and the Italian Space Agency (Agenzia Spaziale Italiana or ASI) aimed at studying the health effects of airborne particulate matter. It combines surface-based air monitoring data and satellite observations to analyze aerosol composition, pollution variability, and in turn potential health impacts. To support ASI research goals, three MAIA primary target areas have been established in Italy. These cover a number of cities including main urban centers in the Po valley such as Milan, Turin, and Bologna.

S4 Tracks of E-EU-03 and E-EU-06 flights

Table S2. Approximate time and location of altitude changes as indicated in Fig.2 in the main text: a) E-EU-03, and b) E-EU-06. Altitudes are given in m above sea level (a.s.l.).

a)

waypoints	date and time (UTC)	(lat. °N, long. °E)	altitude (m)a.s.l.
3a	11.07.2017 10:34	(45.7, 11)	5430
3b	11.07.2017 10:39	(45.6, 10.6)	3530
3c	11.07.2017 10:49	(45.6, 9.6)	3530
3d	11.07.2017 10:51	(45.6, 9.5)	2900
3e	11.07.2017 15:26	(45.6, 11.7)	1010
3f	11.07.2017 15:31	(45.5, 11.8)	3220
3g	11.07.2017 15:39	(45.4, 12.6)	3220

b)

waypoints	date and time (UTC)	(lat. °N, long. °E)	altitude (m)a.s.l.
6	2017-07-20 09:42	(45.5, 13.4)	3200
6a	2017-07-20 09:49	(44.9, 13.5)	3200
6b	2017-07-20 09:53	(45.1, 13.5)	1630
6c	2017-07-20 09:59	(45.5, 13.4)	1630
6d	2017-07-20 10:02	(45.3, 13.4)	520
6e	2017-07-20 10:10	(44.9, 13.4)	520
6f	2017-07-20 10:21	(44.8, 12.6)	520
6g	2017-7-20 10:37	(45.7, 13.2)	520
6h	2017-7-20 10:39	(45.6, 13.1)	1600
6i	2017-7-20 10:54	(44.8, 12.5)	1600
6j	2017-7-20 10:58	(44.9, 12.6)	3220
6k	2017-7-20 11:10	(45.7, 13.2)	3220
6l	2017-7-20 11:19	(45.3, 12.8)	840
6m	2017-7-20 12:07	(44.9, 9)	840
6n	2017-7-20 12:11	(44.6, 9)	2590
6o	2017-7-20 12:19	(44.1, 9)	2590

S5 Distribution of emissions in the Po Plain

The ARPAs (Environmental Protection Regional Agencies) monitor the air quality in the Italian regions by measuring air composition through ground-based stations. In 2017 and 2015, the software INEMAR (INventario EMissioni ARia) and IREA (Inventario Regionale delle Emissioni in Atmosfera, https://servizi.regione.piemonte.it/catalogo/inventario-regionale-delle-emissioni-atmosfera-irea, last access: 05 October 2025) were used to estimate annual emissions of the main macropollutants (CO_2, CO, CH_4, NO_x, N_2O, NH_3, SO_2, VOCs, $PM_{2.5}$ and PM_{10}) from anthropogenic and biogenic sources in the Po Plain regions. The emission sources are divided into 11 groups or macro-sectors based on the international classification EMEP (Cooperative Programme for Monitoring and Evaluation of Long Range Transmission of Air Pollution in Europe) – CORINAIR (CoORdination of Information on the Environment AIR emission)/SNAP (Selected Nomenclature for sources of Air Pollution). The total annual emissions (see Fig. S2) show that the provinces of Milan, Turin and Venice and the south of Lombardy are the main polluted areas. Figure S3 indicates the groups of emissions divided by region, showing that Lombardy is the most polluted region with main emitting groups G1 (Combustion in energy and transformation industry), G2 (Non-industrial combustion processes), G3 (Combustion in manufacturing industry), and G7 (Road transport).

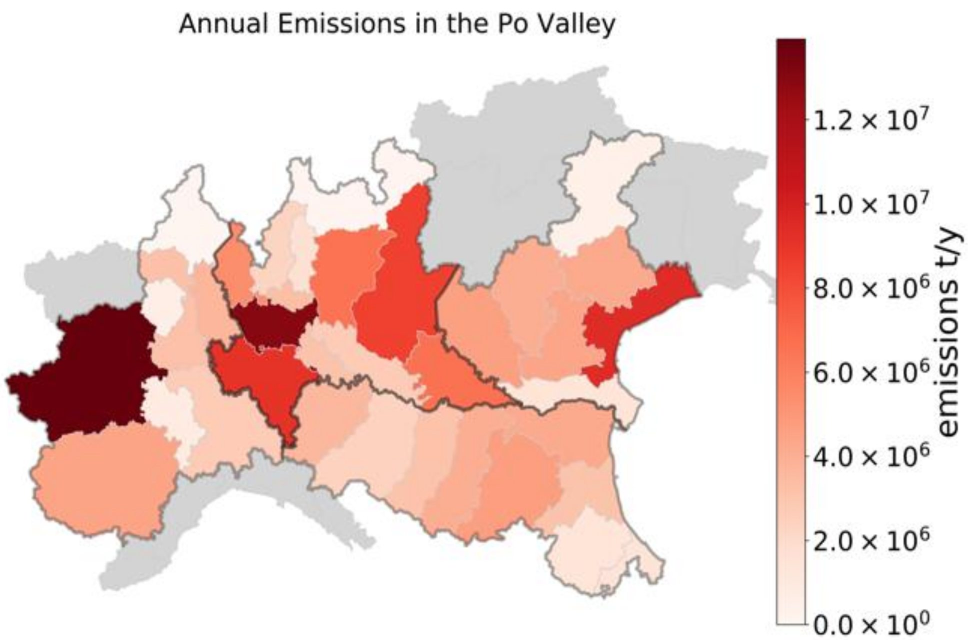

Figure S2. Emissions per province according to the EMEP-CORINAIR/SNAP classification. Data sources: IREA 2015, INEMAR 2017.

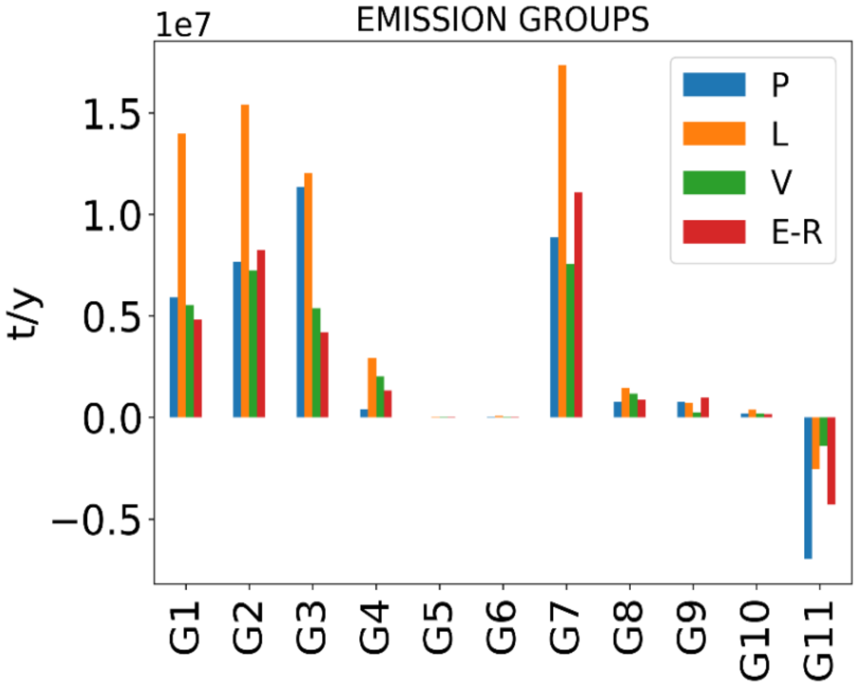

Figure S3. Emissions per region divided into groups of emission according to the EMEP-CORINAIR/SNAP classification. P is Piedmont, L is Lombardy, V is Veneto and E-R is Emilia-Romagna. Groups are: G1: Combustion in energy and transformation industry; G2: Non-industrial combustion processes; G3: Combustion in manufacturing industry; G4: Production processes; G5: Extraction and distribution of fossil fuels and geothermal energy; G6: Solvent and other product use; G7: Road transport; G8: Other mobile sources and machinery; G9: Waste treatment and disposal; G10: Agriculture; G11: Other sources and sinks. Data sources: IREA 2015, INEMAR 2017.

S6 Ground-based stations: ARPA air quality-monitoring network (AQMN) and the ACTRIS Atmospheric Observatory at Ispra.

Table S3. Ground-based stations selected along the flight track of the HALO flights. T: temperature, P: pressure, RH: relative humidity, ws: wind speed; wd: wind direction. Data source: ARPAs' dataset.

station number	station name	station type	measurements	time resolution	(lat. °N, lon. °E)
1	Novi Ligure-Gobetti	Urban traffic	NO, NO_2, NO_x, PM_{10}, ws, wd	Hourly (daily for PM)	(44.76, 8.8)
2	Voghera Pozzoni	Urban background	NO_2, NO_x, O_3, CO, C_6H_6, PM_{10}, ws, wd	Hourly (daily for PM)	(45.0, 9.01)
3	S. Rocco al Porto	Suburban background	NO_2, NO_x, CO, PM_{10}	Hourly (daily for PM)	(45.08, 9.7)
4	Cremona Fatebenefratelli	Urban background	NO_2, NO_x, NH_3, O_3, CO, SO_2, ws, wd	1 hour	(45.14, 10.04)
5	Viadana	Urban background	NO_2, NO_x, O_3	Hourly	(44.92, 10.52)
6	Mantova Gramsci	Urban traffic	NO_2, NO_x, CO, C_6H_6, SO_2, PM_{10}, ws, wd	Hourly (daily for PM)	(45.15, 10.78)
7	Rovigo Centro	Urban traffic	NO_2, O_3, CO, C_6H_6, SO_2, PM_{10}, ws, wd	Hourly (daily for PM)	(45.07, 11.78)
8	Bra- Madonna Fiori	Urban traffic	NO, NO_2, NO_x, PM_{10}, ws, wd	Hourly (daily for PM)	(44.71, 7.84)
9	Vinchio- San Michele	Rural background	NO, NO_2, NO_x, O_3, PM_{10}, $PM_{2.5}$, ws, wd	Hourly (daily for PM)	(44.8, 8.31)
10	Baldissero-Torinese	Rural background	NO, NO_2, NO_x, O_3, CO, ws, wd	Hourly	(45.06, 7.8)
11	Novara- Verdi	Urban background	NO, NO_2, NO_x, O_3, PM_{10}, $PM_{2.5}$, ws, wd	Hourly (daily for PM)	(45.44, 8.62)
12	Saronno Santuario	Urban background	NO_2, NO_x, O_3, PM_{10}, ws, wd	Hourly (daily for PM)	(45.63, 9.04)
13	Sesto San Giovanni	Urban traffic	NO_2, NO_x, CO, $PM_{2.5}$, ws, wd	Hourly (daily for PM)	(45.53, 9.24)
14	Osio Sotto	Suburban background	NO_2, NO_x, O_3, PM_{10}, ws, wd	Hourly (daily for PM)	(45.62, 9.61)
15	Sarezzo	Urban background	NO_2, NO_x, O_3, CO, PM_{10}, ws, wd	Hourly (daily for PM)	(45.65, 10.21)
16	Brescia Via Turati	Urban traffic	NO_2, NO_x, CO, C_6H_6, ws, wd	Hourly	(45.54, 10.23)
17	San Felice	Urban traffic	NO_2, CO, SO_2	Hourly	(45.55, 11.53)

18	Bassano	Urban background	NO_2, O_3, $PM_{2.5}$, ws, wd	Hourly (daily for PM)	(45.76, 11.74)
19	Padova Arcella	Urban traffic	NO_2, CO, PM_{10}, ws, wd	Hourly (daily for PM)	(45.43, 11.89)
20	Genoa_Genova - Quarto	Urban background	NO, NO_2, O_3, SO_2	Hourly	(44.39, 8.99)
21	Genoa_Genova – Corso Firenze	Urban background	NO, NO_2, O_3, CO, SO_2	Hourly	(44.42, 8.93)
22	Genoa_Genova – Via Buozzi	Urban traffic	NO, NO_2, CO, SO_2	Hourly	(44.41, 8.91)
23	Ispra	Rural background	NO, NO_2, O_3, CO, SO_2, PM_{10}, ws, wd, air T, RH, air P, solar radiation	10-minutes	(45.807, 8.631)

Table S4. Ground-based trace gas instrumentation of the ARPA AQMN stations

Species	**Technique/ Instrument**
NO, NO_2, NO_x	Chemiluminescence
CO	Spectrophotometry IR
SO_2	Molecular Fluorescence Spectroscopy
O_3	UV-photometry

S7 LiDAR instruments

Vertical profiles from the following LiDAR systems were considered in this work:

- Automated LiDAR-Ceilometer (ALC) located at the University Milano Bicocca as part of the Italian ALICENET network. It is an OTT_HydroMet (former Lufft) CHM15k-Nimbus working at a single wavelength of 1064 nm, with a 15 s temporal resolution and 15 m vertical resolution. Detailed information on the ALICENET network and data processing are given in Bellini et al. (2024)
- UV LiDAR in San Pietro Capofiume, operated by the University of Naples Federico II (Boselli et al, 2021). It was working at a wavelength of 355 nm, with depolarisation capabilities. The particle backscatter coefficient β_p and particle linear depolarization ratio δ_p profiles were retrieved using the Klett inversion (Klett, 1981). The first valid measurement is at 270 m due to the incomplete overlap between the laser and the field of view of the telescope closer to the surface (Wandinger, 2005).
- LiDAR of the JRC in Ispra, which operates at three different wavelengths: 1064 nm, 532 nm and 355 nm. The βp and the δ_p profiles of the LiDAR in Ispra have been retrieved using the ACTRIS-EARLINET (Aerosol, Clouds and Trace Gases Research Infrastructure-European Aerosol Research Lidar Network) Single Calculus Chain (https://www.earlinet.org, last access: 05 October 2025).

S8 Average mixing ratios and ratios between species measured during E-EU-06 over the Po Plain

Table S5: Mean (mean), standard deviation (std) and quartiles (25th, 50th, 75th) mixing ratios and concentrations of selected measured species (a, b), and ratios between trace gases and aerosols (c) for the E-EU-06 flight over the Po Plain. Note that RO_2^* is defined in the main text and HCHO and NO_2 are remote measurements by the mini-DOAS instrument. BC, NO_3^-, SO_4^{2-} are given for standard temperature and pressure conditions. The periods within the BL are marked in yellow and in blue are the averages calculated within the BL over the CPP. The position of the shuttles B-C and F-G are also shown in a) for clarification (see main text)

a)

		B-C				F-G				
flight legs		6-6a	6b-6c	6d-6e	6e-6f	6f-6g	6h-6i	6j-6k	6l-6m	6n-6o
time		09:39 09:48	09:53 10:00	10:02 10:10	10:10 10:20	10:21 10:37	10:39 10:54	10:57 11:10	11:19 12:06	12:10 12:19
altitude (m)	mean	**3229**	**1626**	**516**	**522**	**519**	**1631**	**3229**	**836**	**2579**
	std	2	2	1	3	4	6	2	4	47
CO (ppb)	mean	**83**	**135**	**126**	**131**	**122**	**109**	**79**	**120**	**80**
	std	1	3	4	10	7	15	1	8	2
	25th	82	134	123	122	116	92	78	114	79
	50th	83	135	125	135	123	111	79	120	80
	75th	84	137	129	137	126	121	80	126	82
SO_2 (ppt)	mean	**115**	**669**	**1895**	**1094**	**978**	**269**	**143**	**991**	**116**
	std	21	80	1025	391	327	158	21	512	19
	25th	100	611	1342	959	687	169	131	640	104
	50th	114	664	1671	1068	979	193	145	827	115
	75th	126	723	2090	1224	1197	318	157	1143	128
NO (ppb)	mean	**0.05**	**0.20**	**0.27**	**0.27**	**0.21**	**0.16**	**0.09**	**0.49**	**0.04**
	std	0.00	0.08	0.07	0.12	0.09	0.03	0.03	0.29	0.01
	25th	0.05	0.13	0.25	0.18	0.17	0.14	0.07	0.28	0.04
	50th	0.05	0.20	0.28	0.26	0.20	0.16	0.07	0.45	0.05
	75th	0.06	0.26	0.32	0.33	0.22	0.18	0.13	0.58	0.05
NO_2 (ppt)	mean	**80**	**204**	**378**	**472**	**426**	**136**	**98**	**1014**	**131**
	std	5	11	49	45	53	30	10	468	14
	25th	77	200	335	438	390	106	92	655	122
	50th	80	206	360	470	421	137	96	875	130
	75th	83	210	430	501	469	165	102	1329	138
NO_y (ppb)	mean	**0.5**	**7.2**	**3.0**	**6**	**4.1**	**3.5**	**0.9**	**7**	**1.1**
	std	0.0	0.4	0.7	1	0.9	2	0.1	3	0.2
	25th	0.5	6.9	2.6	5	3.3	2	0.9	5	1.0
	50th	0.5	7.1	2.8	6	3.7	4	0.9	6	1.1
	75th	0.6	7.3	3.2	7	4.7	5	1.0	9	1.2
O_3 (ppb)	mean	**51**	**91**	**75**	**79**	**74**	**67**	**51**	**72**	**55**
	std	0.3	4	3	5	3	13	1	5	2
	25th	50	89	73	74	72	54	51	69	54
	50th	51	92	74	81	74	69	51	73	55
	75th	51	93	77	83	75	77	52	75	56

b)

flight legs		6-6a	6b-6c	6d-6e	6e-6f	6f-6g	6h-6i	6j-6k	6l-6m	6n-6o
time		09:39 09:48	09:53 10:00	10:02 10:10	10:10 10:20	10:21 10:37	10:39 10:54	10:57 11:10	11:19 12:06	12:10 12:19
altitude (m)	**mean**	**3229**	**1626**	**516**	**522**	**519**	**1631**	**3229**	**836**	**2579**
	std	2	2	1	3	4	6	2	4	47
RO_2^* (ppt)	**mean**	**65**	**88**	**86**	**103**	**90**	**84**	**64**	**61**	**45**
	std	6	8	8	11	10	20	3	18	13
	25th	61	81	81	97	86	70	62	49	38
	50th	64	89	85	100	92	81	62	58	44
	75th	67	95	91	108	97	93	64	74	48
HCHO (ppt)	**mean**	**648**	**1299**	**1639**	**1919**	**1613**	**1046**	**541**	**1806**	**544**
	std	32	51	93	118	204	151	38	337	35
	25th	613	1256	1571	1844	1415	876	509	1563	520
	50th	655	1325	1610	1932	1558	1117	550	1722	533
	75th	674	1336	1732	1991	1801	1163	561	2048	574
C_3H_6O (ppt)	**mean**	**1661**	**3205**	**2626**	**3437**	**2752**	**2332**	**1703**	**3002**	**1726**
	std	69	189	78	367	307	379	94	354	60
	25th	1639	3030	2576	3396	2574	2016	1668	2788	1703
	50th	1652	3292	2580	3503	2640	2122	1721	3053	1723
	75th	1695	3321	2709	3564	2946	2724	1756	3260	1757
NO_3^- ($\mu g m^{-3}$)	**mean**	**0.1**	**5.4**	**0.21**	**2**	**0.3**	**1.5**	**0.06**	**2**	**0.06**
	std	0.0	0.6	0.08	1	0.4	1.5	0.02	1	0.02
	25th	0.1	5.0	0.15	1	0.1	0.1	0.05	1	0.05
	50th	0.1	5.4	0.16	2	0.2	1.1	0.06	1	0.06
	75th	0.1	5.6	0.27	3	0.2	2.3	0.07	2	0.07
SO_4^{2-} ($\mu g m^{-3}$)	**mean**	**0.6**	**2.0**	**2.2**	**1.9**	**2.5**	**1.3**	**0.62**	**1.7**	**0.64**
	std	0.0	0.1	0.4	0.3	1.0	0.5	0.05	0.4	0.09
	25th	0.6	2.0	2.0	1.8	1.6	0.8	0.57	1.4	0.60
	50th	0.6	2.0	2.2	1.9	2.2	1.2	0.61	1.5	0.65
	75th	0.6	2.1	2.4	2.0	3.2	1.6	0.64	1.9	0.68
BC ($\mu g m^{-3}$)	**mean**	**0.1**	**0.4**	**0.4**	**0.4**	**0.4**	**0.2**	**0.09**	**0.4**	**0.08**
	std	0.1	0.1	0.1	0.1	0.1	0.1	0.06	0.1	0.05
	25th	0.1	0.3	0.3	0.4	0.3	0.1	0.06	0.3	0.05
	50th	0.1	0.4	0.4	0.4	0.4	0.2	0.07	0.4	0.07
	75th	0.1	0.4	0.4	0.5	0.4	0.3	0.10	0.5	0.09

c)

flight legs		6-6a	6b-6c	6d-6e	6e-6f	6f-6g	6h-6i	6j-6k	6l-6m	6n-6o
time		09:39 09:48	09:53 10:00	10:02 10:10	10:10 10:20	10:21 10:37	10:39 10:54	10:57 11:10	11:19 12:06	12:10 12:19
altitude (m)	**mean**	**3229**	**1626**	**516**	**522**	**519**	**1631**	**3229**	**836**	**2579**
	std	2	2	1	3	4	6	2	4	47
NO_y/CO	**mean**	**0.007**	**0.053**	**0.024**	**0.044**	**0.033**	**0.030**	**0.012**	**0.057**	**0.014**
	std	0.000	0.003	0.005	0.007	0.007	0.010	0.002	0.023	0.002
	25th	0.006	0.052	0.021	0.038	0.027	0.018	0.011	0.039	0.013
	50th	0.006	0.053	0.022	0.046	0.032	0.033	0.011	0.051	0.014
	75th	0.007	0.054	0.026	0.049	0.038	0.038	0.013	0.072	0.015
NO_y/NO_2	**mean**	**7**	**35**	**8**	**12**	**9**	**24**	**10**	**7**	**9**
	std	1	3	1	2	1	7	2	2	1
	25th	6	33	7	10	8	17	9	6	8
	50th	7	35	8	13	9	25	10	7	8
	75th	7	37	9	14	10	28	11	8	9
HCHO/CO	**mean**	**0.0078**	**0.010**	**0.013**	**0.015**	**0.013**	**0.010**	**0.007**	**0.015**	**0.007**
	std	0.0004	0.000	0.001	0.001	0.002	0.001	0.001	0.003	0.000
	25th	0.0074	0.009	0.012	0.014	0.012	0.009	0.006	0.013	0.006
	50th	0.0078	0.010	0.013	0.015	0.013	0.010	0.007	0.015	0.007
	75th	0.0081	0.010	0.014	0.015	0.014	0.010	0.007	0.018	0.007
$HCHO/NO_2$	**mean**	**8.12**	**6.38**	**4.36**	**4.09**	**3.81**	**7.85**	**5.54**	**2.04**	**4.23**
	std	0.63	0.47	0.36	0.31	0.29	0.76	0.46	0.64	0.58
	25th	7.69	6.15	4.05	3.92	3.65	7.11	5.15	1.56	3.85
	50th	8.12	6.32	4.44	4.07	3.85	7.87	5.59	2.00	4.26
	75th	8.60	6.47	4.63	4.25	3.99	8.39	5.88	2.49	4.57
SO_2/CO	**mean**	**0.001**	**0.005**	**0.015**	**0.008**	**0.008**	**0.003**	**0.002**	**0.008**	**0.001**
	std	0.000	0.001	0.008	0.003	0.003	0.001	0.000	0.004	0.000
	25th	0.001	0.005	0.011	0.007	0.006	0.002	0.002	0.005	0.001
	50th	0.001	0.005	0.014	0.008	0.008	0.002	0.002	0.007	0.001
	75th	0.002	0.005	0.017	0.009	0.009	0.003	0.002	0.009	0.002
CO/BC	**mean**	**693**	**314**	**351**	**312**	**346**	**625**	**710**	**315**	**898**
	std	45	18	46	52	46	270	63	55	137
	25th	648	305	309	299	317	390	680	271	809
	50th	705	309	348	304	344	510	690	311	898
	75th	734	318	396	310	358	890	717	356	963
NO_3^- /BC	**mean**	**0.9**	**13**	**0.6**	**4**	**0.8**	**5**	**0.7**	**4**	**0.7**
	std	0.3	2	0.2	3	0.6	4	0.2	2	0.3
	25th	0.7	11	0.4	2	0.4	1	0.5	2	0.5
	50th	0.8	12	0.6	3	0.5	5	0.6	3	0.7
	75th	0.9	13	0.7	7	0.8	8	0.8	5	0.9
SO_4^{2-}/BC	**mean**	**6.3**	**5.0**	**5.9**	**4.1**	**7**	**7**	**6.9**	**4**	**8**
	std	0.6	0.3	0.6	0.8	3	1	0.8	1	2
	25th	5.8	4.9	5.7	3.9	4	5	6.5	3	7
	50th	6.3	5.0	6.0	4.2	6	6	6.7	4	8
	75th	6.9	5.0	6.2	4.4	8	8	7.3	5	9
Organics/BC	**mean**	**13**	**15**	**10**	**10**	**9**	**20**	**10**	**9**	**15**
	std	2	1	1	2	1	4	2	2	5
	25th	12	14	9	9	8	17	9	8	13
	50th	13	15	10	11	9	18	10	9	14
	75th	14	15	10	11	10	23	12	10	18

S9 Average mixing ratios and ratios between species measured in the CPP for P1 to P8 during E-EU-06

Table S6: Mean (mean), standard deviation (std) and quartiles (25th, 50th, 75th) of a-b) concentrations and, c) ratios between selected species for the P1 to P8 periods during the E-EU-06 flight over the CPP. Note that RO_2^* is defined in the main text and HCHO and NO_2 are remote measurements by the mini DOAS instrument. BC, NO_3^-, SO_4^{2-} are given for standard temperature and pressure conditions. The averages calculated within the BL over the whole CPP (6l-6m, marked in yellow) are additionally shown. The periods defined as local and temporary background periods are coloured in blue.

a)

flight periods		P1	P2	P3	P4	P5	P6	P7	P8	6l-6m
time		11:26 11:32	11:32 11:35	11:36 11:39	11:40 11:43	11:43 11:52	11:53 11:57	11:58 12:02	12:03 12:07	11:19 12:06
altitude (m)	mean	**839**	**840**	**839**	**838**	**834**	**833**	**833**	**834**	**836**
	std	2	2	2	2	2	2	2	3	4
CO (ppb)	mean	**128**	**110**	**120**	**126**	**114**	**119**	**126**	**110**	**120**
	std	7	5	7	9	4	2	2	4	8
	25th	125	106	113	121	111	118	125	107	114
	50th	129	110	120	127	114	119	127	109	120
	75th	135	114	125	132	116	121	127	112	126
SO_2 (ppt)	mean	**771**	**559**	**1025**	**701**	**759**	**1882**	**1529**	**566**	**991**
	std	181	139	342	129	211	518	497	107	512
	25th	665	471	763	626	609	1458	1078	500	640
	50th	776	573	1075	707	714	1864	1425	549	827
	75th	883	650	1247	782	839	2300	1961	625	1143
NO (ppb)	mean	**0.29**	**0.19**	**0.43**	**0.59**	**0.46**	**0.62**	**1.11**	**0.50**	**0.49**
	std	0.06	0.05	0.05	0.16	0.07	0.09	0.24	0.04	0.29
	25th	0.25	0.16	0.39	0.46	0.42	0.54	1.00	0.47	0.28
	50th	0.30	0.20	0.44	0.64	0.45	0.62	1.05	0.48	0.45
	75th	0.34	0.23	0.48	0.72	0.50	0.71	1.17	0.51	0.58
NO_2 (ppt)	mean	**680**	**738**	**905**	**1457**	**1019**	**1408**	**1867**	**745**	**1014**
	std	83	39	129	240	187	271	174	211	468
	25th	628	720	797	1298	875	1151	1766	617	655
	50th	669	742	917	1425	977	1407	1895	653	875
	75th	724	754	1017	1706	1117	1620	1988	808	1329
NO_y (ppb)	mean	**5.9**	**4.0**	**7.5**	**9.8**	**6.1**	**9.1**	**12.1**	**4.3**	**7**
	std	0.9	0.8	1.6	2.4	1.1	0.8	2.5	0.5	3
	25th	5.3	3.5	6.5	8.2	5.5	8.6	10.3	4.0	5
	50th	6.0	4.1	7.3	10.2	6.1	8.9	12.1	4.2	6
	75th	6.6	4.7	8.7	11.9	6.7	9.8	13.9	4.4	9
O_3 (ppb)	mean	**74**	**69**	**71**	**72**	**72**	**74**	**67**	**61**	**72**
	std	3	2	2	3	2	2	4	2	5
	25th	74	68	70	70	71	73	65	60	69
	50th	75	69	71	73	72	75	68	60	73
	75th	76	70	73	74	74	75	70	62	75

b)

flight periods		P1	P2	P3	P4	P5	P6	P7	P8	6l-6m
time		11:26 11:32	11:32 11:35	11:36 11:39	11:40 11:43	11:43 11:52	11:53 11:57	11:58 12:02	12:03 12:07	11:19 12:06
altitude (m)	mean	**839**	**840**	**839**	**838**	**834**	**833**	**833**	**834**	**836**
	std	2	2	2	2	2	2	2	3	4
RO_2^* (ppt)	mean	**67**	**63**	**41**	**37**	**53**	**53**	**60**	**88**	**61**
	std	8	5	5	8	5	14	23	3	18
	25th	61	60	39	33	50	47	52	86	49
	50th	70	62	43	38	51	53	66	87	58
	75th	72	65	44	41	54	63	74	89	74
HCHO (ppt)	mean	**1557**	**1591**	**1612**	**1824**	**1813**	**2201**	**2464**	**1888**	**1806**
	std	86	69	56	40	125	49	212	215	337
	25th	1467	1529	1563	1808	1722	2159	2166	1643	1563
	50th	1587	1535	1611	1828	1763	2197	2550	1814	1722
	75th	1601	1657	1627	1843	1838	2248	2628	2037	2048
C_3H_6O (ppt)	mean	**3499**	**2798**	**3491**	**2670**	**2816**	**3050**	**3002**	**2372**	**3002**
	std	119	396			292	175	133	64	354
	25th	3440	2597	3491	2670	2686	2946	2965	2343	2788
	50th	3530	2783	3491	2670	2802	3078	3031	2383	3053
	75th	3555	2993	3491	2670	2954	3182	3068	2407	3260
NO_3^- (μgm^{-3})	mean	**1.7**	**0.7**	**3.1**	**3.7**	**1.1**	**2.0**	**2.4**	**0.1**	**2**
	std	0.6	0.4	1.5	1.8	0.5	0.4	0.9	0.0	1.2
	25th	1.4	0.5	2.6	3.7	0.8	1.8	1.9	0.1	0.7
	50th	1.7	0.6	2.9	4.6	1.0	2.0	2.6	0.1	1.4
	75th	2.2	1.0	4.0	4.8	1.4	2.2	3.0	0.1	2.2
SO_4^{2-} (μgm^{-3})	mean	**1.9**	**1.4**	**1.6**	**1.3**	**1.4**	**1.9**	**1.4**	**1.6**	**1.7**
	std	0.3	0.1	0.2	0.1	0.1	0.2	0.1	0.1	0.4
	25th	1.6	1.4	1.5	1.3	1.3	1.8	1.3	1.6	1.4
	50th	1.9	1.5	1.6	1.4	1.4	1.9	1.4	1.6	1.5
	75th	2.2	1.5	1.7	1.4	1.4	1.9	1.5	1.6	1.9
BC (μgm^{-3})	mean	**0.5**	**0.3**	**0.5**	**0.5**	**0.3**	**0.4**	**0.5**	**0.3**	**0.4**
	std	0.1	0.1	0.1	0.2	0.1	0.1	0.2	0.1	0.1
	25th	0.4	0.2	0.4	0.4	0.3	0.3	0.4	0.2	0.3
	50th	0.5	0.3	0.4	0.5	0.3	0.4	0.5	0.3	0.4
	75th	0.6	0.4	0.5	0.6	0.4	0.4	0.6	0.3	0.5

c)

flight periods		P1	P2	P3	P4	P5	P6	P7	P8	6l-6m
time		11:26 11:32	11:32 11:35	11:36 11:39	11:40 11:43	11:43 11:52	11:53 11:57	11:58 12:02	12:03 12:07	11:19 12:06
altitude (m)	mean	**839**	**840**	**839**	**838**	**834**	**833**	**833**	**834**	**836**
	std	2	2	2	2	2	2	2	3	4
NO_y/CO	mean	**0.046**	**0.037**	**0.057**	**0.078**	**0.054**	**0.076**	**0.095**	**0.039**	**0.057**
	std	0.006	0.006	0.005	0.017	0.009	0.006	0.019	0.003	0.023
	25th	0.042	0.032	0.054	0.070	0.049	0.072	0.081	0.037	0.039
	50th	0.046	0.037	0.057	0.078	0.053	0.075	0.095	0.039	0.051
	75th	0.049	0.042	0.060	0.090	0.058	0.081	0.110	0.040	0.072
NO_y/NO_2	mean	**8.8**	**5.5**	**9.4**	**7.1**	**6.1**	**7.0**	**6.4**	**6.0**	**7.1**
	std	1.9	1.0	2.1	2.4	1.1	1.5	1.0	1.1	2.0
	25th	7.7	4.6	7.8	4.7	5.4	5.6	5.4	5.4	5.6
	50th	8.4	5.5	9.6	7.8	6.1	7.4	6.5	6.1	6.9
	75th	10.1	6.3	10.8	9.0	6.8	8.1	7.2	6.5	8.2
HCHO/CO	mean	**0.012**	**0.015**	**0.014**	**0.015**	**0.016**	**0.018**	**0.020**	**0.017**	**0.015**
	std	0.001	0.001	0.001	0.001	0.001	0.000	0.002	0.001	0.003
	25th	0.012	0.014	0.013	0.014	0.015	0.018	0.017	0.015	0.013
	50th	0.012	0.014	0.014	0.014	0.016	0.019	0.020	0.017	0.015
	75th	0.013	0.015	0.015	0.015	0.016	0.019	0.021	0.018	0.018
$HCHO/NO_2$	mean	**2.34**	**2.16**	**1.81**	**1.29**	**1.83**	**1.63**	**1.34**	**2.65**	**2.04**
	std	0.26	0.10	0.24	0.22	0.30	0.32	0.21	0.48	0.64
	25th	2.20	2.08	1.60	1.06	1.61	1.33	1.15	2.34	1.56
	50th	2.39	2.19	1.76	1.29	1.85	1.56	1.37	2.67	2.00
	75th	2.55	2.24	1.98	1.41	2.03	1.95	1.48	2.94	2.49
SO_2/CO	mean	**0.006**	**0.005**	**0.007**	**0.006**	**0.007**	**0.016**	**0.012**	**0.005**	**0.008**
	std	0.001	0.001	0.002	0.001	0.002	0.004	0.004	0.001	0.004
	25th	0.005	0.004	0.005	0.005	0.005	0.012	0.009	0.005	0.005
	50th	0.006	0.005	0.007	0.006	0.006	0.016	0.011	0.005	0.007
	75th	0.007	0.006	0.009	0.006	0.007	0.019	0.016	0.006	0.009
CO/BC	mean	**271**	**323**	**282**	**277**	**353**	**312**	**253**	**421**	**315**
	std	32	51	24	26	20	20	16	21	55
	25th	261	295	268	268	344	310	244	410	271
	50th	270	311	277	288	356	311	252	421	311
	75th	272	345	292	292	363	321	262	431	356
NO_3^- /BC	mean	**3.2**	**2.8**	**5.6**	**6.5**	**3.2**	**5.2**	**4.1**	**0.5**	**3.7**
	std	0.5	0.4	2.4	2.2	1.0	0.3	2.3	0.0	2.1
	25th	3.0	2.6	4.5	5.4	2.4	5.0	2.8	0.5	2.4
	50th	3.2	2.8	5.9	6.4	3.1	5.2	4.6	0.5	3.3
	75th	3.5	3.0	6.8	7.6	3.8	5.4	5.9	0.5	5.0
SO_4^{2-}/BC	mean	**3.6**	**4.3**	**3.4**	**2.9**	**4.3**	**4.9**	**2.8**	**6.0**	**4.4**
	std	0.5	0.9	0.1	0.3	0.3	0.6	0.4	0.6	1.4
	25th	3.3	3.8	3.3	2.8	4.1	4.7	2.5	5.8	3.3
	50th	3.7	3.9	3.3	3.0	4.3	5.0	2.6	6.3	4.1
	75th	3.9	4.6	3.4	3.1	4.5	5.2	2.8	6.4	5.2
Organics/BC	mean	**7.5**	**9.9**	**8.3**	**8.8**	**10.4**	**10.5**	**7.0**	**9.4**	**9.3**
	std	0.7	1.8	0.1	1.0	0.6	0.7	0.8	0.4	1.9
	25th	7.2	9.0	8.2	8.2	9.9	9.9	6.6	9.2	8.1
	50th	7.5	9.7	8.2	8.4	10.3	10.4	6.8	9.2	9.4
	75th	8.0	10.7	8.3	9.1	10.7	11.0	7.2	9.5	10.4

S10 Meteorological data over the Po Plain

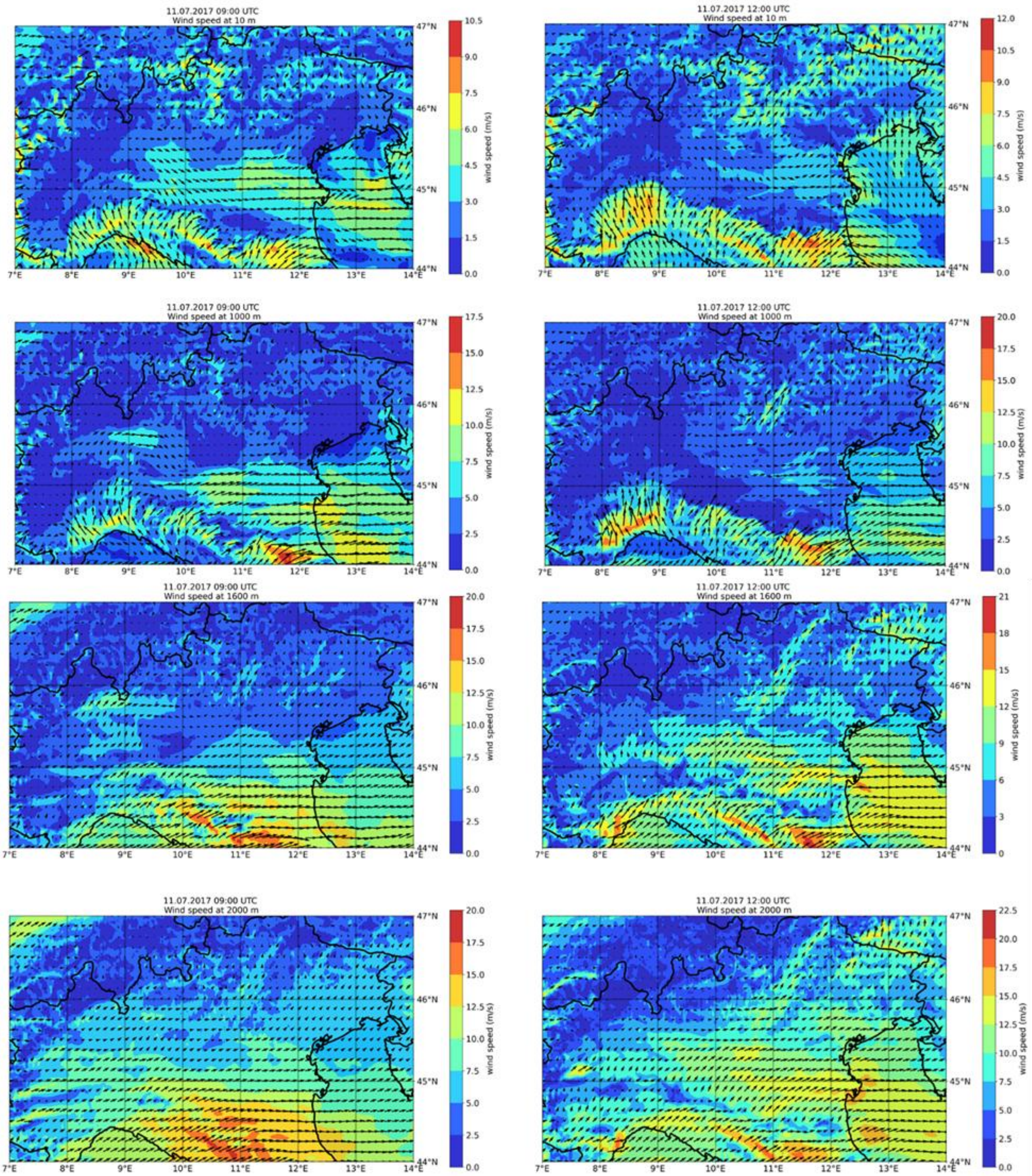

Figure S4. Wind simulation over the Po Plain by COSMO on 11 July.2017 at 9 UTC (left) and 12 UTC (right) for 10 m, 1000 m, 1600 m, and 2000 m altitude a.s.l. Please note changes in the scale of the wind speed.

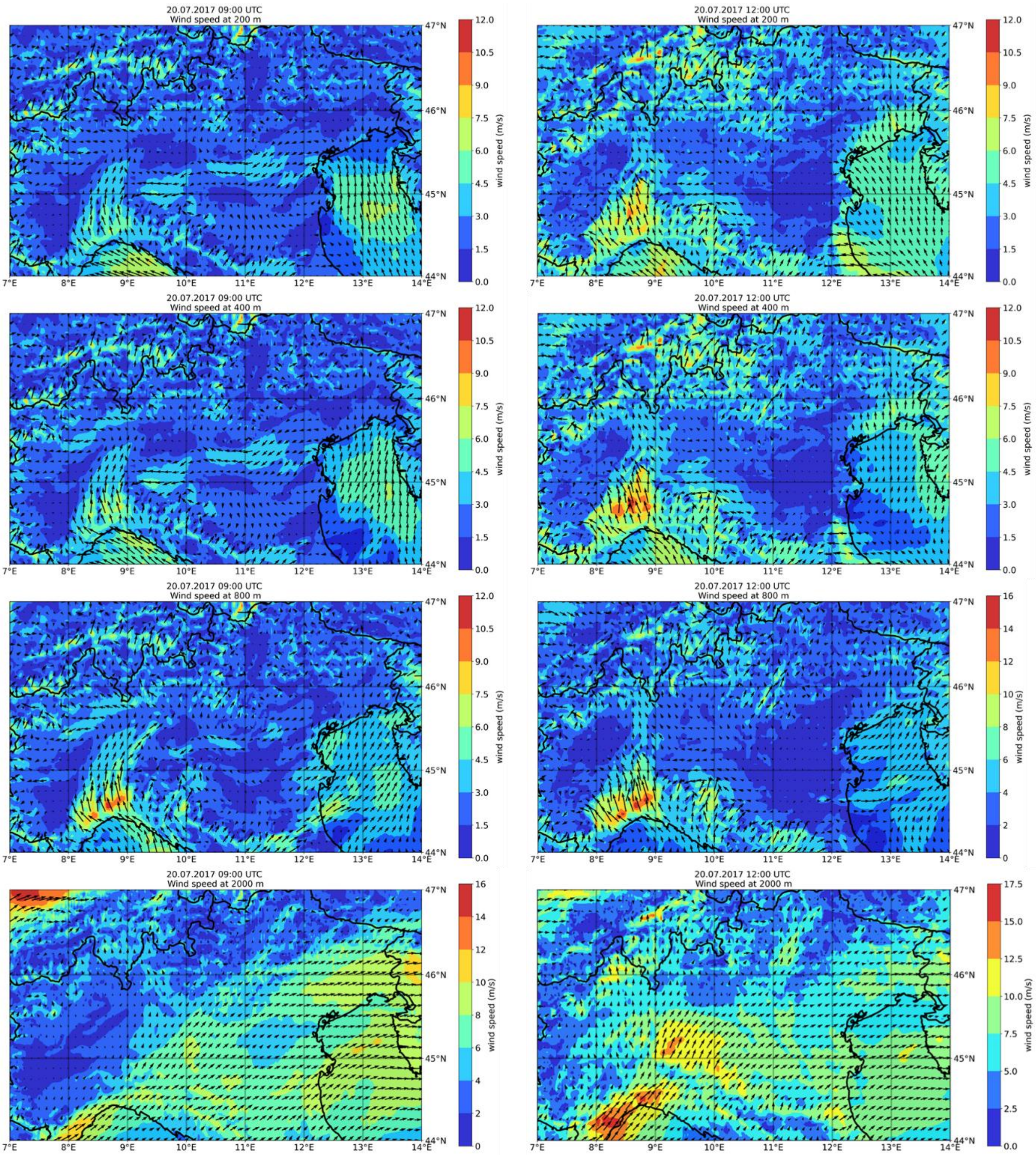

Figure S5. Wind simulation over the Po Plain by COSMO on 20 July 2017 at 9 UTC (left) and 12 UTC (right) for 200 m, 400 m, 800 m, and 2000 m altitude a.s.l. Please note the changes in the scale of the wind speed.

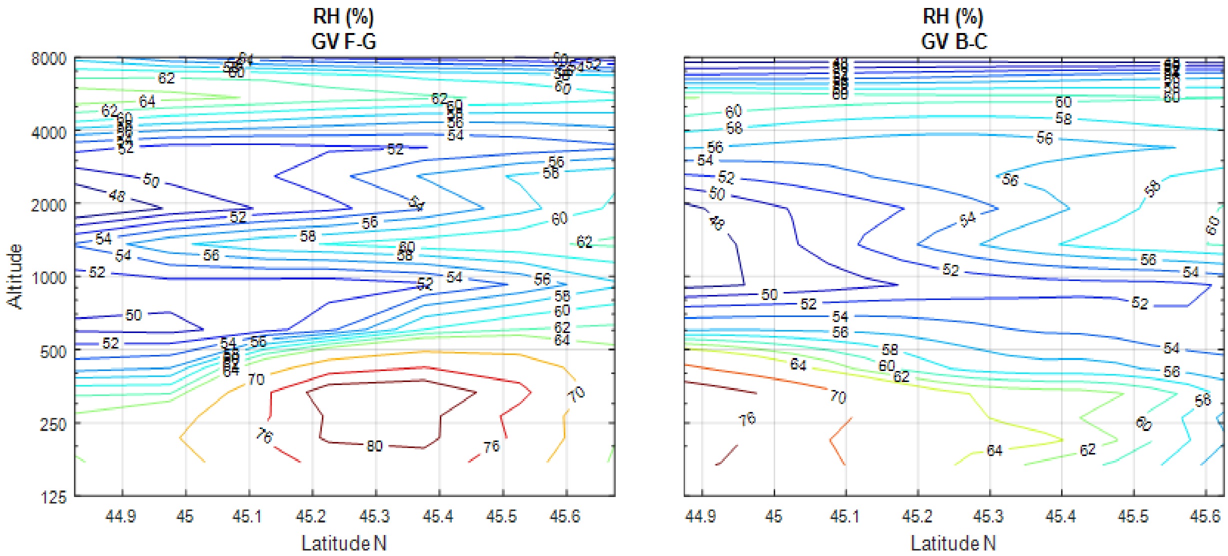

Figure S6. Relative humidity profiles along the F-G (left-hand) and B-C (right hand) flight track: meteorological reanalysis generated by the EMEP MSC-W model (Simpson et al., 2012) in hindcast mode.

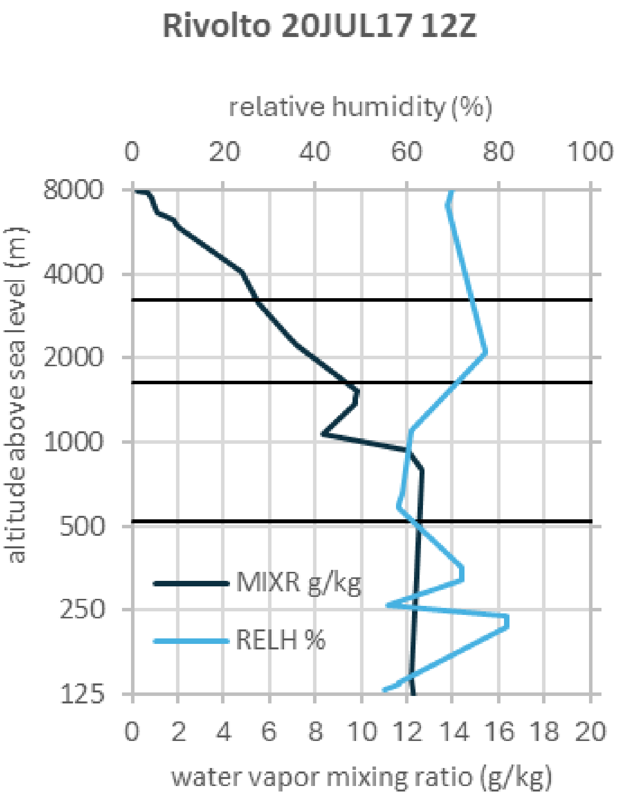

Figure S7. Relative humidity and water vapor mixing ratio profiles measured by the radiosonde at Rivolto (45.97 °N, 13.05 °E) on 20 July 2017 at 12 UTC.

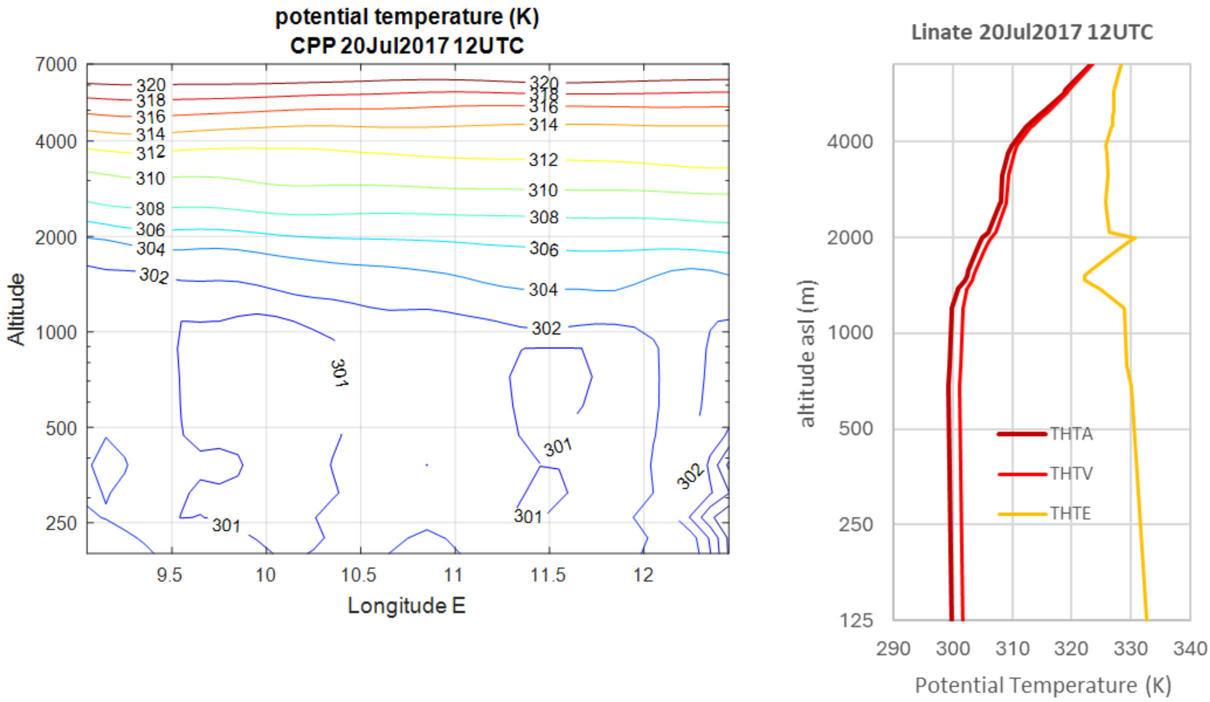

Figure S8. Potential temperature profiles along the transect across the Central Po Plain at 45 °N (meteorological reanalysis generated by the EMEP MSC-W model in hindcast mode), and measured by the radiosonde at Milan-Linate (45.43 °N, 9.28 °E) on 20 July 2017 at 12 UTC. THTA= potential temperature, THTV= virtual potential temperature, THTE= equivalent potential temperature.

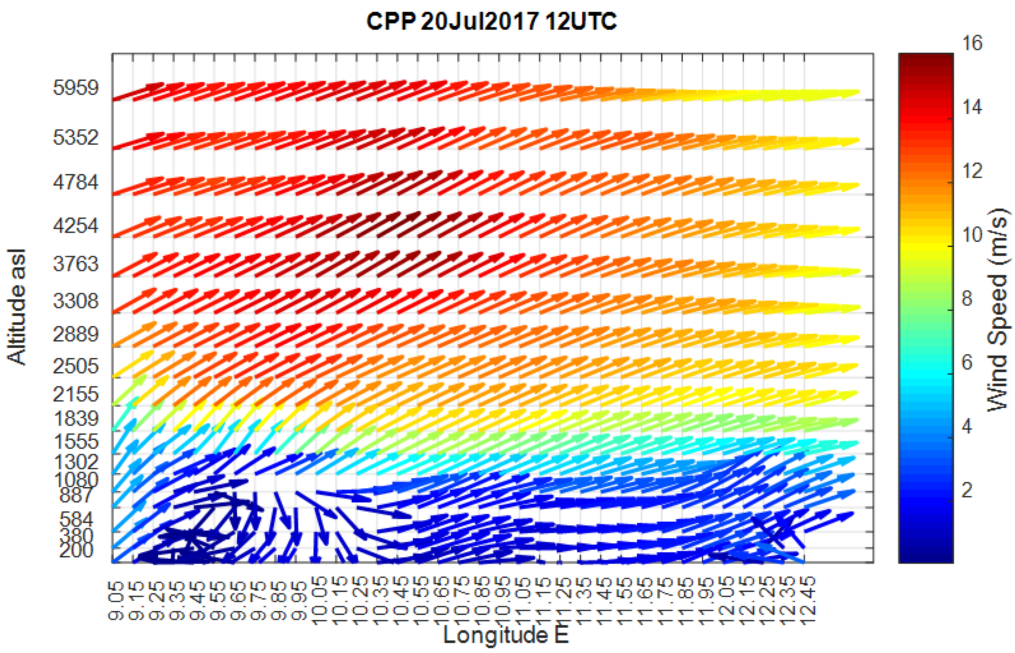

Figure S9. Wind profile along the transect across the Central Po Plain at 45 °N: meteorological reanalysis generated by the EMEP MSC-W model (Simpson et al., 2012) in hindcast mode.

S11 Backward FLEXTRA trajectories for the shuttles during E-EU-06 flight on the 20 July 2017

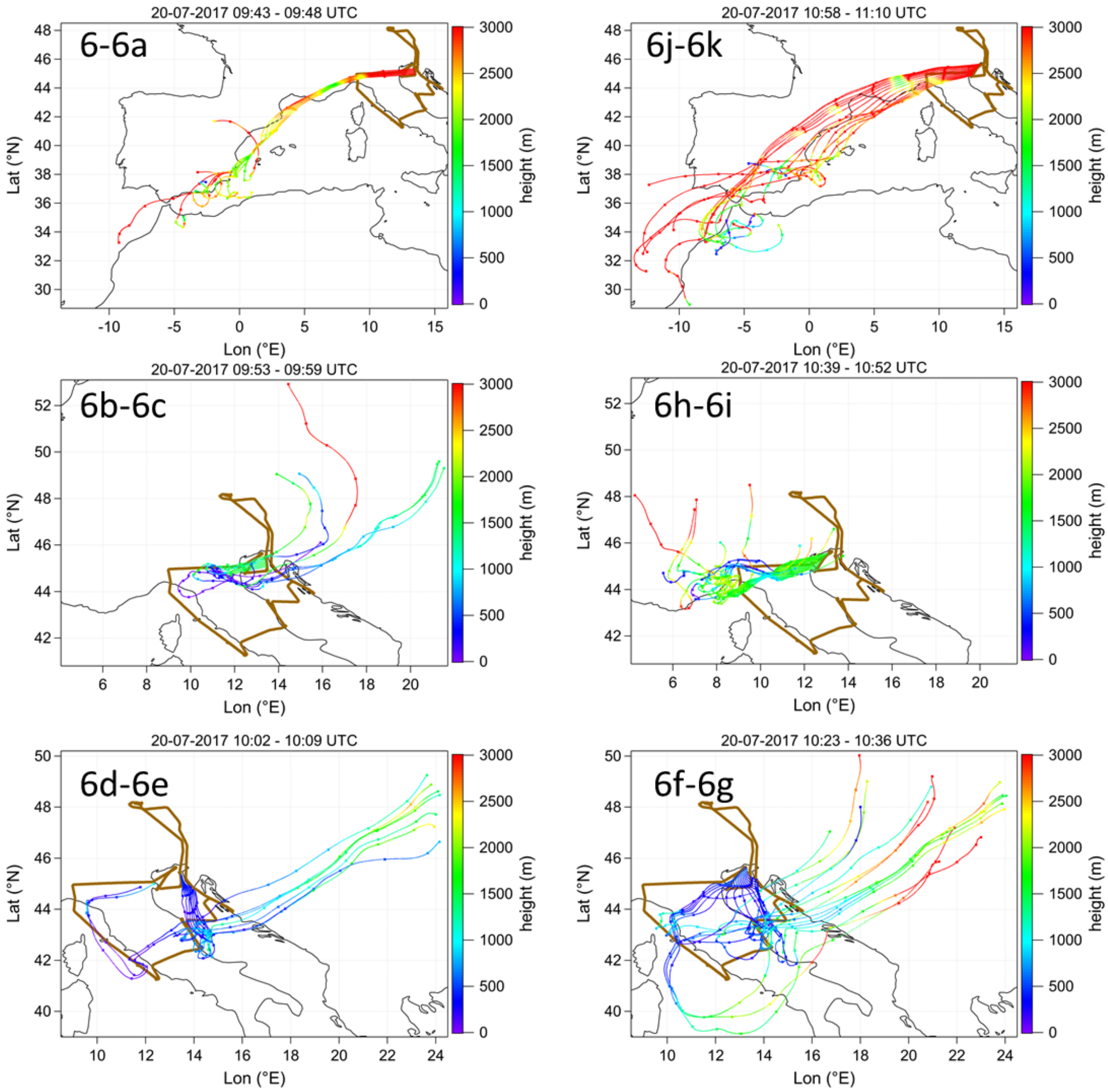

Figure S10. Ninety-six hours FLEXTRA backward trajectories for the first (left panel) and second (right panel) shuttles during the E-EU-06 flight. The waypoints for each level of the shuttle are indicated in each graph. The trajectories are started every two minutes at the HALO altitude within the time intervals indicated on the top of each graph. Dots mark the 6h time steps along each trajectory. The flight track is indicated in brown.

S12 FLEXTRA and LAGRANTO back trajectories and COSMO-LAGRANTO wind field

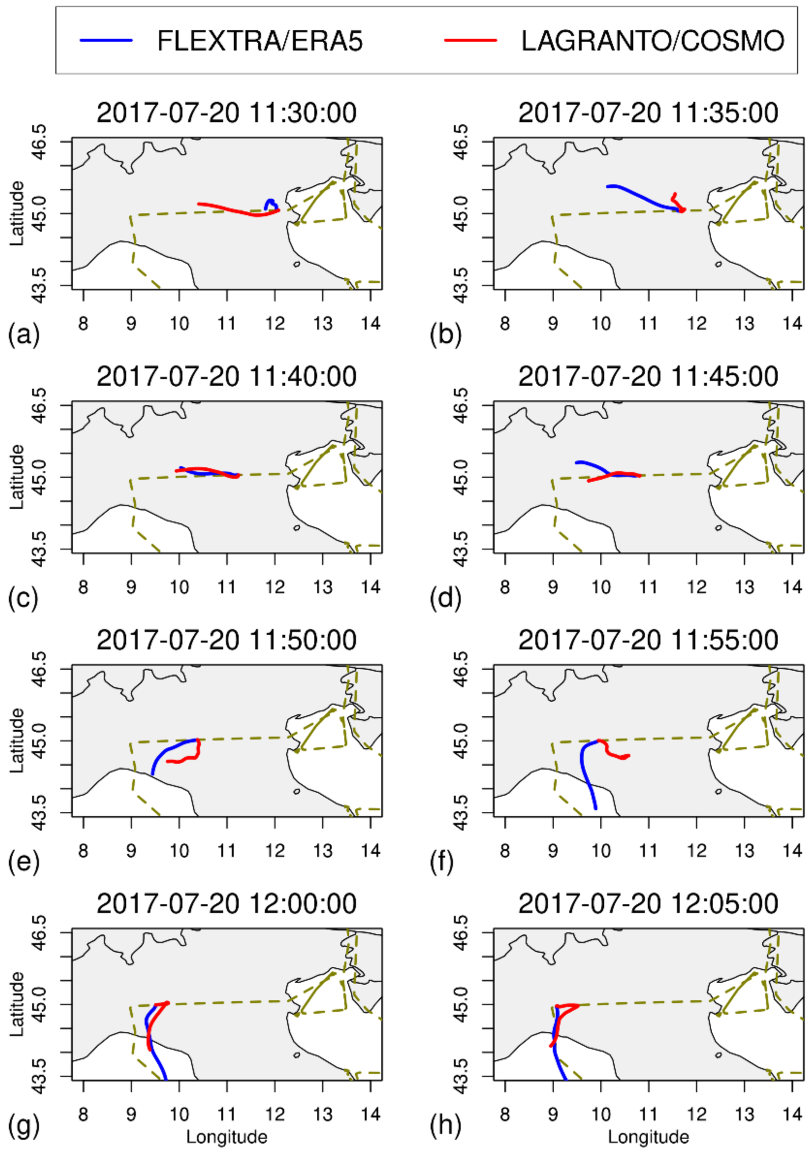

Figure S11. Comparison between FLEXTRA (blue) and COSMO-LAGRANTO 12-hours back-trajectories (red) for the track over the CPP during the E-EU-06 flight. Back-trajectories are exemplary calculated every 5 minutes starting from the aircraft coordinates.

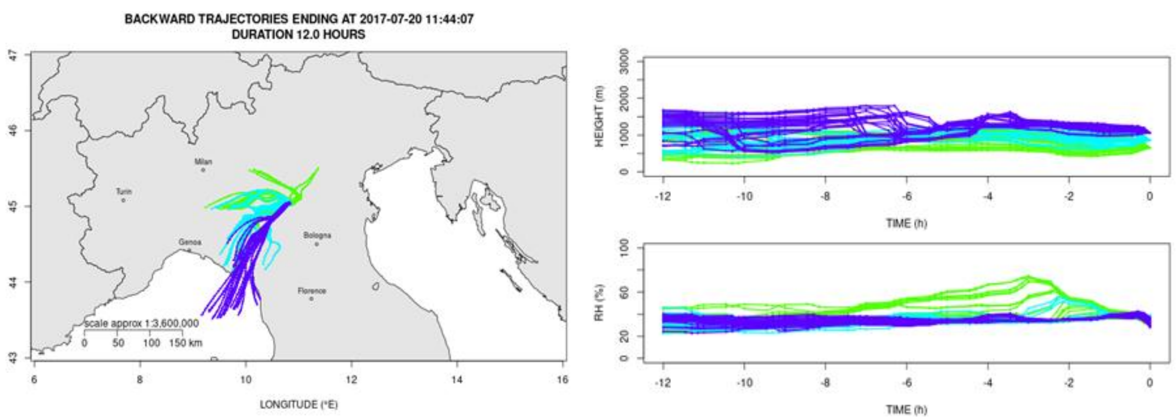

Figure S12. COSMO-LAGRANTO 12-hours back-trajectories from a selected point of the E-EU-06 flight track. Back-trajectories start inside a 2-km diameter circle at three different altitudes (green: HALO altitude – 200m, blue: HALO altitude of 840 m, purple: HALO altitude + 200m).

S13 HYSPLIT forward trajectories

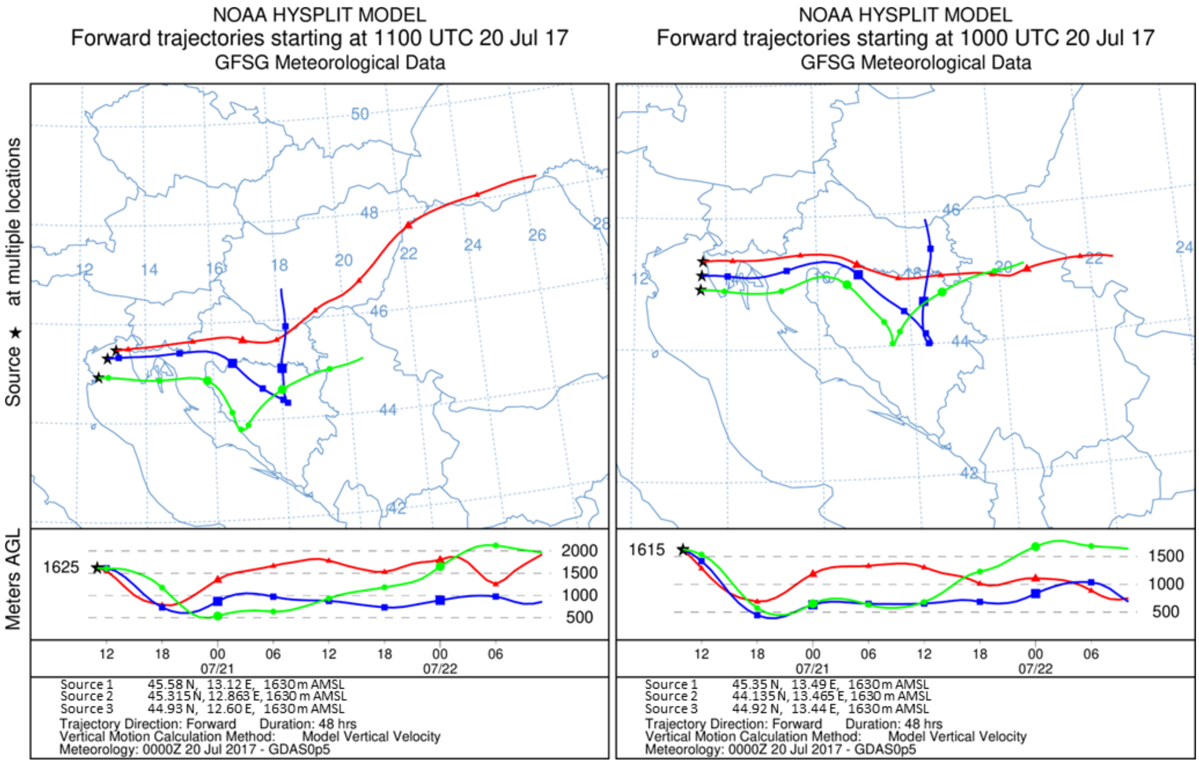

Figure S13. HYSPLIT 48-hr forward trajectories showing the export of the polluted air masses probed in GV at 1630 m a.s.l across B-C (6b-6c, right panel) and F-G (6i-6h, left panel).

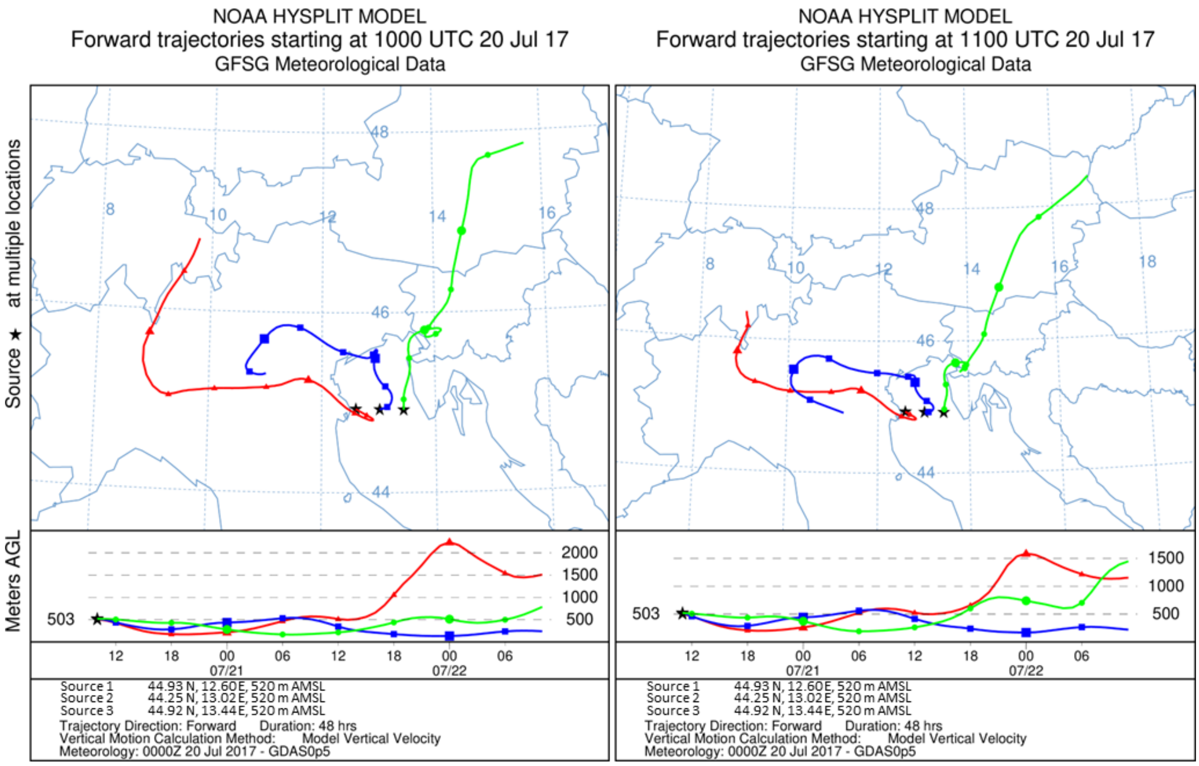

Figure S14. HYSPLIT 48-hr forward trajectories showing the return and export of the polluted air masses probed in GV at 520 m asl across B-F (6e-6f) at 10:00 UTC (left panel) and 11:00 UTC (right panel).

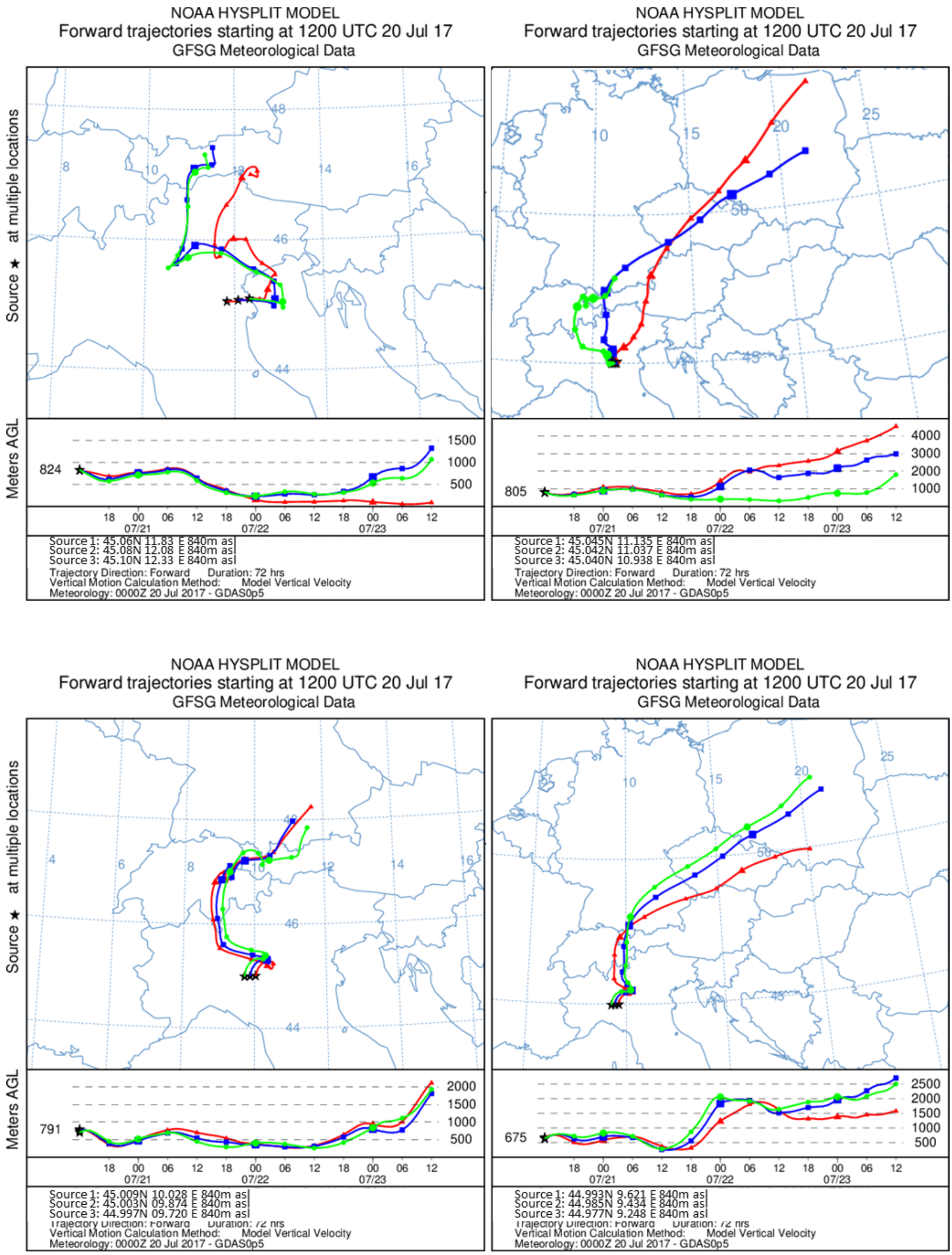

Figure S15. HYSPLIT 72-hr forward trajectories showing the return and export of the pollution plumes probed in CPP at 840 m a.s.l during periods P1, P4, P6 and P7.

S14 Vertical profiles by LiDAR and Ceilometers in the central Po Plain area

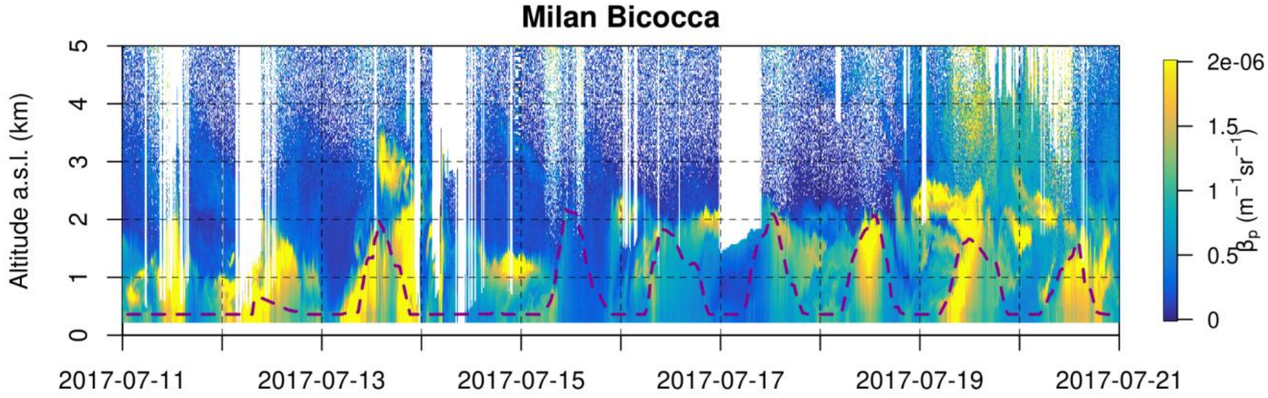

Figure S16. Continuous (0-24 UTC, x-axis) vertical profiles (0-5 km, y-axis) of aerosol backscatter at 1064 nm as observed by the ALICENET ALC system operating in Milan-Bicocca from July 11 to July 20, 2017. Cloud-affected profiles are filtered out from the cloud base upwards (white areas). The dashed line is the height of the Mixed Aerosol Layer (MAL) as derived from the ALICENET data processing (Bellini et al., 2024); it is artificially set to zero when persistence of clouds prevented the MAL retrieval.

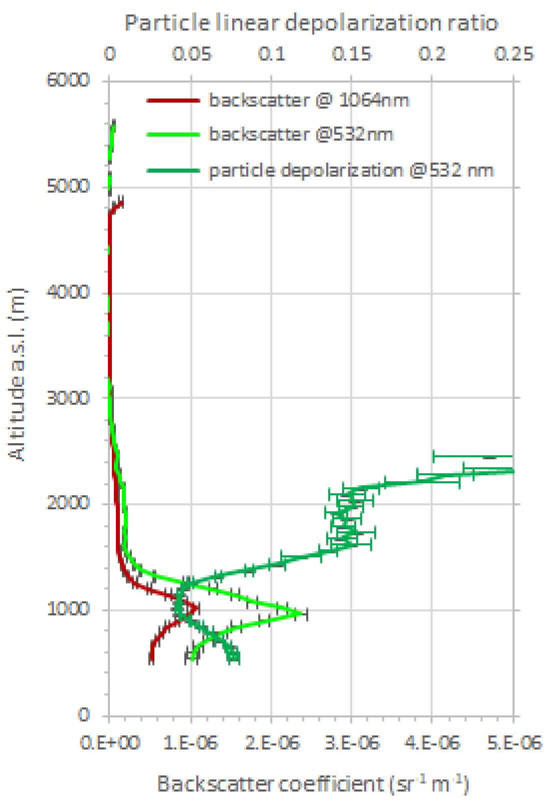

Figure S17. Vertical profiles of the particle light backscatter coefficient at 1064 and 532 nm, and the linear depolarization ratio at 532 nm measured by the LiDAR in Ispra on the 11 July at 10:17-10:42 UTC

S15 Multi-Model Ensemble Desert Dust forecasts for the 20 July 2017

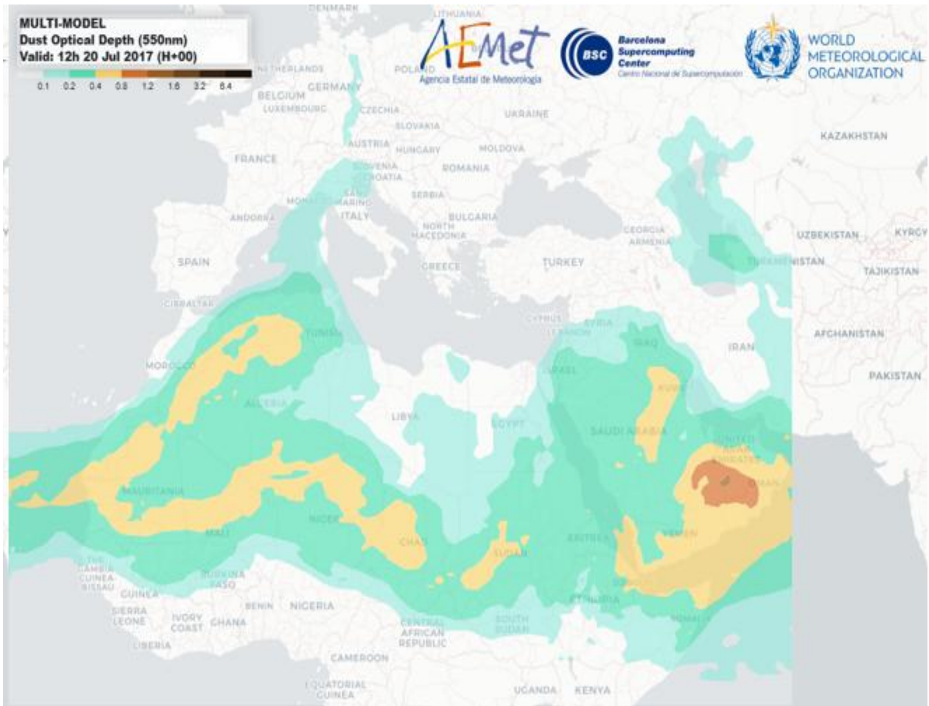

Figure S18. Dust Optical Depth at 550 nm derived from the Multi-model Ensemble at 12 UTC (i.e., approximately at the HALO overpass time) for July 20 2017, showing an optically thin desert dust layer advected over Northern Italy (credits: WMO Barcelona Dust Regional Center and the SDS-WAS)

References

Ambrosetti, P., Anfossi, D., Cieslik, S., Graziani, G., Lamprecht, R., Marzorati, A., Nodop, K.,Sandroni, S., Stingele, A., and Zimmermann, H.: Mesoscale transport of atmospheric trace constituents across the central alps: TRANSALP tracer experiments. Atmos. Environ. 32 (7), 1257–1272, doi: 10.1016/S1352-2310(97)00185-4, 1998.

Apituley, A. Alves Gouveia, D., den Hoed, M. et al.: Research Infrastructures Services Reinforcing Air Quality Monitoring Capacities in European Urban & Industrial AreaS (GA n. 101036245), https://riurbans.eu/wp-content/uploads/2024/04/RI-URBANS_D32_D4_11.pdf (last access 01 June 2026), 2024.

Baklanov A., Mahura A. (Eds.): Interactions between Air Quality and Meteorology, Deliverable D4.3, MEGAPOLI Scientific Report 10-10, MEGAPOLI-13-REP-2010-03, 48p, ISBN: 978-87-993898-3-4, 2010.

Belis, C., Blond, N., Bouland, C., Carnevale, C., Clappier, A., Douros, J., Fragkou, E., Guariso, G., Miranda, A. I., Nahorski, Z., Pisoni, E., Ponche, J.-L., Thunis, P., Viaene, P., and Volta, M.: Strengths and Weaknesses of the Current EU Situation. Springer International Publishing, pp. 69–83., doi: 10.1007/978-3-319-33349-6_4, 2017.

Bellini, A., Diémoz, H., Di Liberto, L., Gobbi, G. P., Bracci, A., Pasqualini, F., and Barnaba, F.: ALICENET – an Italian network of automated lidar ceilometers for four-dimensional aerosol monitoring: infrastructure, data processing, and applications, Atmos. Meas. Tech., 17, 6119–6144, https://doi.org/10.5194/amt-17-6119-2024, 2024.

Boselli A. de Marco, C., Mocerino, L., Murena, F., Quaranta, F., Rizzuto, E., Sannino, A., Spinelli, N.,and Xuan, W.: Evaluating LIDAR Sensors for the Survey of Emissions from Ships at Harbor. In: Okada T., Suzuki K., Kawamura Y. (eds) Practical Design of Ships and Other Floating Structures. PRADS 2019. Lecture Notes in Civil Engineering, vol 64. Springer, Singapore. https://doi.org/10.1007/978-981-15-4672-3_49, 2021.

Diner, D.J., Boland, S.W., Brauer, M., Bruegge, C., Burke, K.A., Chipman, R., Di Girolamo, L., Garay, M.J., Hasheminassab, S., Hyer, E., Jerrett, M., Jovanovic, V., Kalashnikova, O.V., Liu, Y., Lyapustin, A.I., Martin, R.V., Nastan, A., Ostro, B.D., Ritz, B., Schwartz, J., Wang, J., Xu,, F.: Advances in multiangle satellite remote sensing of speciated airborne particulate matter and association with adverse health effects: from MISR to MAIA, J. Appl. Remote Sens. 12(4), 042603, doi: 10.1117/1.JRS.12.042603, 2018.

Dosio, A., Galmarini, S. and Graziani G. : Simulation of the circulation and related photochemical ozone dispersion in the Po plains (northern Italy): Comparison with the observations of a measuring campaign. Environment Institute, Joint Research Center, Ispra, Italy, doi: 10.1029/2000JD000046, 2002.

Gauss, M. and the CityZen Team: CityZen: megaCITY – Zoom for the Environment, Project Final Report, European Commission, Grant Agreement No. 212095, available at: europa.eu (last access: 1 June 2026), 2011.

Klett, J.D.: Stable analytical inversion solution for processing lidar returns, Applied Optics, Vol. 20, No. 2 , 1981.

Magnani,C., Renzi, L., Paglione, M, Rinaldi, M., Petit, J. E., Timonen, H., Zannoni H, N., Mazzini, M. and A. Marinoni: One year of aerosol chemical composition and source apportionment in Milan. SIF Congress 2023 - 09th Meeting of the Italian Physical Society, Salerne, Italy. pp.264, ⟨10.1393/ncc/i2024-24264-y⟩. ⟨hal-04836025⟩, 2023.

Marongiu, A., Angelino, E., Moretti, M., Malvestiti, G. and Fossati, G.: Atmospheric Emission Sources in the Po-Basin from the LIFE-IP PREPAIR Project. Open Journal of Air Pollution, 11, 70-83. https://doi.org/10.4236/ojap.2022.113006, 2022.

Neftel, A., Spirig, C., Prévôt, A. S. H., Furger, M., Stutz, J., Vogel, B., and Hjorth, J.: Sensitivity of photooxidant production in the Milan Basin: An overview of results from a EUROTRAC-2 Limitation of Oxidant Production field experiment. J. Geophys. Res., 107(D22), 8188, doi: 10.1029/2001JD001263, 2002.

Raffaelli, K., Deserti, M., Stortini, M., Amorati, R., Vasconi, M., and Giovannini, G.: Improving Air Quality in the Po Valley, Italy: Some Results by the LIFE-IP-PREPAIR Project, Atmosphere 11, 429, doi: 10.3390/atmos11040429, 2020.

Rotach, M. W., Serafin, S., Ward, H. C., Arpagaus, M., Colfescu, I., Cuxart, J., De Wekker, S.F.J., Grubišic,V, Kalthoff, N., Karl, T., Kirshbaum, D.J., Lehner, M., Mobbs, S., Paci, A., Palazzi, E., Bailey, A., Schmidli, J., Wittmann, C., Wohlfahrt, G., and Zardi, D.: A Collaborative Effort to Better Understand, Measure, and Model Atmospheric Exchange Processes over Mountains. Bull. Amer. Meteor. Soc., 103, E1282–E1295, https://doi.org/10.1175/BAMS-D-21-0232.1, 2022.

Simpson, D., Benedictow, A., Berge, H., Bergström, R., Emberson, L. D., Fagerli, H., Flechard, C. R., Hayman, G. D., Gauss, M., Jonson, J. E., Jenkin, M. E., Nyíri, A., Richter, C., Semeena, V. S., Tsyro, S., Tuovinen, J.-P., Valdebenito, Á., and Wind, P.: The EMEP MSC-W chemical transport model – technical description, Atmos. Chem. Phys., 12, 7825–7865, https://doi.org/10.5194/acp-12-7825-2012, 2012.

Wandinger, U.: Introduction to lidar. In Lidar: range-resolved optical remote sensing of the atmosphere (pp. 1-18). New York, NY: Springer New York, 2005.